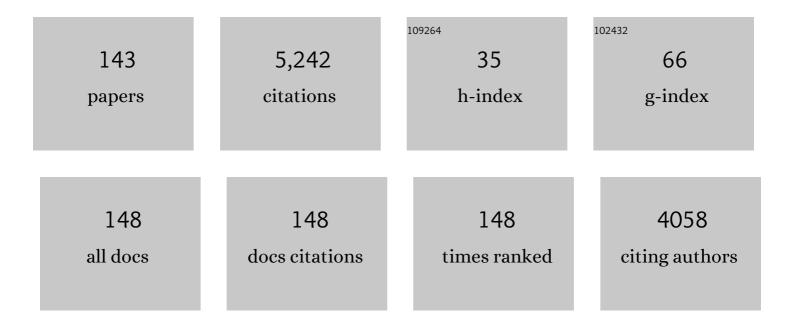
List of Publications by Year in descending order

Source: https://exaly.com/author-pdf/2994996/publications.pdf Version: 2024-02-01



#	Article	IF	CITATIONS
1	Interfacial reactions between lead-free solders and common base materials. Materials Science and Engineering Reports, 2005, 49, 1-60.	14.8	971
2	Impurity and alloying effects on interfacial reaction layers in Pb-free soldering. Materials Science and Engineering Reports, 2010, 68, 1-38.	14.8	288
3	Piezoelectric coefficients and spontaneous polarization of ScAlN. Journal of Physics Condensed Matter, 2015, 27, 245901.	0.7	209
4	Cycle aging of commercial NMC/graphite pouch cells at different temperatures. Applied Energy, 2015, 154, 160-172.	5.1	191
5	Reactive sputter deposition and properties of TaxN thin films. Microelectronic Engineering, 2002, 64, 289-297.	1.1	144
6	Hybrid carbon based nanomaterials for electrochemical detection of biomolecules. Progress in Materials Science, 2017, 88, 499-594.	16.0	137
7	Thermodynamics, Diffusion and the Kirkendall Effect in Solids. , 2014, , .		132
8	Growth Mechanism and Origin of High <mml:math <br="" xmlns:mml="http://www.w3.org/1998/Math/MathML">display="inline"><mml:mi>s</mml:mi><mml:msup><mml:mi>p</mml:mi><mml:mn>3</mml:mn></mml:msup> Content in Tetrahedral Amorphous Carbon. Physical Review Letters, 2018, 120, 166101.</mml:math>	:/m and: mat	h>128
9	Effect of Ag, Fe, Au and Ni on the growth kinetics of Sn–Cu intermetallic compound layers. Microelectronics Reliability, 2009, 49, 242-247.	0.9	94
10	Formation of Intermetallic Compounds Between Liquid Sn and Various CuNi x Metallizations. Journal of Electronic Materials, 2008, 37, 792-805.	1.0	92
11	Electrochemical Fouling of Dopamine and Recovery of Carbon Electrodes. Analytical Chemistry, 2018, 90, 1408-1416.	3.2	84
12	Failure mechanism of Ta diffusion barrier between Cu and Si. Journal of Applied Physics, 2000, 88, 3377-3384.	1.1	82
13	Heat generation in high power prismatic Li-ion battery cell with LiMnNiCoO ₂ cathode material. International Journal of Energy Research, 2014, 38, 1424-1437.	2.2	78
14	Reactivity of Amorphous Carbon Surfaces: Rationalizing the Role of Structural Motifs in Functionalization Using Machine Learning. Chemistry of Materials, 2018, 30, 7446-7455.	3.2	77
15	Solid-State Reactions between Cu(Ni) Alloys and Sn. Journal of Electronic Materials, 2007, 36, 1355-1362.	1.0	74
16	Computational Surface Chemistry of Tetrahedral Amorphous Carbon by Combining Machine Learning and Density Functional Theory. Chemistry of Materials, 2018, 30, 7438-7445.	3.2	69
17	Evolution of microstructure and failure mechanism of lead-free solder interconnections in power cycling and thermal shock tests. Microelectronics Reliability, 2007, 47, 1135-1144.	0.9	68
18	Understanding X-ray Spectroscopy of Carbonaceous Materials by Combining Experiments, Density Functional Theory, and Machine Learning. Part I: Fingerprint Spectra. Chemistry of Materials, 2019, 31, 9243-9255.	3.2	62

#	Article	IF	CITATIONS
19	Electrochemical reactions of catechol, methylcatechol and dopamine at tetrahedral amorphous carbon (ta-C) thin film electrodes. Diamond and Related Materials, 2015, 59, 30-39.	1.8	59
20	Carbon nanotube (CNT) forest grown on diamond-like carbon (DLC) thin films significantly improves electrochemical sensitivity and selectivity towards dopamine. Sensors and Actuators B: Chemical, 2015, 211, 177-186.	4.0	52
21	Phase formation between lead-free Sn–Ag–Cu solder and Ni(P)â^•Au finishes. Journal of Applied Physics, 2006, 99, 023530.	1.1	51
22	Electron transport determines the electrochemical properties of tetrahedral amorphous carbon (ta-C) thin films. Electrochimica Acta, 2017, 225, 1-10.	2.6	49
23	Understanding X-ray Spectroscopy of Carbonaceous Materials by Combining Experiments, Density Functional Theory, and Machine Learning. Part II: Quantitative Fitting of Spectra. Chemistry of Materials, 2019, 31, 9256-9267.	3.2	49
24	Tantalum carbide and nitride diffusion barriers for Cu metallisation. Microelectronic Engineering, 2002, 60, 71-80.	1.1	47
25	TaC as a diffusion barrier between Si and Cu. Journal of Applied Physics, 2002, 91, 5391-5399.	1.1	46
26	New electrochemically improved tetrahedral amorphous carbon films for biological applications. Diamond and Related Materials, 2014, 49, 62-71.	1.8	45
27	Reactive Phase Formation in Thin Film Metal/Metal and Metal/Silicon Diffusion Couples. Critical Reviews in Solid State and Materials Sciences, 2003, 28, 185-230.	6.8	44
28	Unmodified and multi-walled carbon nanotube modified tetrahedral amorphous carbon (ta-C) films as in vivo sensor materials for sensitive and selective detection of dopamine. Biosensors and Bioelectronics, 2018, 118, 23-30.	5.3	44
29	Machine learning driven simulated deposition of carbon films: From low-density to diamondlike amorphous carbon. Physical Review B, 2020, 102, .	1.1	44
30	Correlation between sp ³ -to-sp ² Ratio and Surface Oxygen Functionalities in Tetrahedral Amorphous Carbon (ta-C) Thin Film Electrodes and Implications of Their Electrochemical Properties. Journal of Physical Chemistry C, 2016, 120, 8298-8304.	1.5	43
31	Reliability of Lead-Free Solder Interconnections in Thermal and Power Cycling Tests. IEEE Transactions on Components and Packaging Technologies, 2009, 32, 302-308.	1.4	41
32	Atomic and electronic structure of tetrahedral amorphous carbon surfaces from density functional theory: Properties and simulation strategies. Carbon, 2014, 77, 1168-1182.	5.4	41
33	Nanodiamonds on tetrahedral amorphous carbon significantly enhance dopamine detection and cell viability. Biosensors and Bioelectronics, 2017, 88, 273-282.	5.3	41
34	Chemical stability of Ta diffusion barrier between Cu and Si. Thin Solid Films, 2000, 373, 64-67.	0.8	39
35	Trifluoroacetylazobenzene for optical and electrochemical detection of amines. Journal of Materials Chemistry A, 2015, 3, 4687-4694.	5.2	38
36	Accurate schemes for calculation of thermodynamic properties of liquid mixtures from molecular dynamics simulations. Journal of Chemical Physics, 2016, 145, 244504.	1.2	38

#	Article	IF	CITATIONS
37	Integrated Carbon Nanostructures for Detection of Neurotransmitters. Molecular Neurobiology, 2015, 52, 859-866.	1.9	37
38	Analysis of the redeposition of AuSn4 on Ni/Au contact pads when using SnPbAg, SnAg, and SnAgCu solders. Journal of Electronic Materials, 2005, 34, 103-111.	1.0	34
39	Simultaneous Detection of Morphine and Codeine in the Presence of Ascorbic Acid and Uric Acid and in Human Plasma at Nafion Single-Walled Carbon Nanotube Thin-Film Electrode. ACS Omega, 2019, 4, 17726-17734.	1.6	33
40	Electrochemical Detection of Oxycodone and Its Main Metabolites with Nafion-Coated Single-Walled Carbon Nanotube Electrodes. Analytical Chemistry, 2020, 92, 8218-8227.	3.2	31
41	Diamond-like carbon (DLC) thin film bioelectrodes: Effect of thermal post-treatments and the use of Ti adhesion layer. Materials Science and Engineering C, 2014, 34, 446-454.	3.8	30
42	SU-8 based pyrolytic carbon for the electrochemical detection of dopamine. Journal of Materials Chemistry B, 2017, 5, 9033-9044.	2.9	30
43	Multiwalled Carbon Nanotubes/Nanofibrillar Cellulose/Nafion Composite-Modified Tetrahedral Amorphous Carbon Electrodes for Selective Dopamine Detection. Journal of Physical Chemistry C, 2019, 123, 24826-24836.	1.5	30
44	Simultaneous electrochemical detection of tramadol and O-desmethyltramadol with Nafion-coated tetrahedral amorphous carbon electrode. Electrochimica Acta, 2019, 295, 347-353.	2.6	30
45	Trends in Carbon, Oxygen, and Nitrogen Core in the X-ray Absorption Spectroscopy of Carbon Nanomaterials: A Guide for the Perplexed. Journal of Physical Chemistry C, 2021, 125, 973-988.	1.5	30
46	Diffusion and growth mechanism of Nb3Sn superconductor grown by bronze technique. Applied Physics Letters, 2010, 96, .	1.5	29
47	Disposable Nafion-Coated Single-Walled Carbon Nanotube Test Strip for Electrochemical Quantitative Determination of Acetaminophen in a Finger-Prick Whole Blood Sample. Analytical Chemistry, 2020, 92, 13017-13024.	3.2	29
48	Simulation of dynamic recrystallization in solder interconnections during thermal cycling. Computational Materials Science, 2010, 50, 690-697.	1.4	28
49	Carbon thin films as electrode material in neural sensing. Surface and Coatings Technology, 2014, 259, 33-38.	2.2	28
50	Effect of Ni content on the diffusion-controlled growth of the product phases in the Cu(Ni)–Sn system. Philosophical Magazine, 2016, 96, 15-30.	0.7	28
51	Single-Walled Carbon Nanotube Network Electrodes for the Detection of Fentanyl Citrate. ACS Applied Nano Materials, 2020, 3, 1203-1212.	2.4	28
52	Effect of oxygen on the reactions in the Si/Ta/Cu metallization system. Journal of Materials Research, 2001, 16, 2939-2946.	1.2	27
53	Carbon Nanostructure Based Platform for Enzymatic Glutamate Biosensors. Journal of Physical Chemistry C, 2017, 121, 4618-4626.	1.5	27
54	Partially Reduced Graphene Oxide Modified Tetrahedral Amorphous Carbon Thin-Film Electrodes as a Platform for Nanomolar Detection of Dopamine. Journal of Physical Chemistry C, 2017, 121, 8153-8164.	1.5	26

#	Article	IF	CITATIONS
55	Structural morphology of carbon nanofibers grown on different substrates. Carbon, 2016, 98, 343-351.	5.4	25
56	Amorphous layer formation at the TaC/Cu interface in the Si/TaC/Cu metallization system. Applied Physics Letters, 2002, 80, 938-940.	1.5	24
57	Combined Thermodynamic-Kinetic Analysis of the Interfacial Reactions between Ni Metallization and Various Lead-Free Solders. Materials, 2009, 2, 1796-1834.	1.3	23
58	Evaluation of the surface free energy of spin-coated photodefinable epoxy. Journal of Polymer Science, Part B: Polymer Physics, 2002, 40, 2137-2149.	2.4	22
59	Thermodynamic reassessment of Au–Ni–Sn ternary system. Calphad: Computer Coupling of Phase Diagrams and Thermochemistry, 2013, 43, 61-70.	0.7	22
60	Glutamate detection by amino functionalized tetrahedral amorphous carbon surfaces. Talanta, 2015, 141, 175-181.	2.9	22
61	Pt-grown carbon nanofibers for enzymatic glutamate biosensors and assessment of their biocompatibility. RSC Advances, 2018, 8, 35802-35812.	1.7	22
62	Accurate Computational Prediction of Core-Electron Binding Energies in Carbon-Based Materials: A Machine-Learning Model Combining Density-Functional Theory and <i>GW</i> . Chemistry of Materials, 2022, 34, 6240-6254.	3.2	22
63	Determination of diffusion parameters and activation energy of diffusion in V3Si phase with A15 crystal structure. Scripta Materialia, 2009, 60, 377-380.	2.6	21
64	Application-Specific Catalyst Layers: Pt-Containing Carbon Nanofibers for Hydrogen Peroxide Detection. ACS Omega, 2017, 2, 496-507.	1.6	21
65	Selective detection of morphine in the presence of paracetamol with anodically pretreated dual layer Ti/tetrahedral amorphous carbon electrodes. Electrochemistry Communications, 2018, 86, 166-170.	2.3	21
66	Integrating Carbon Nanomaterials with Metals for Bio-sensing Applications. Molecular Neurobiology, 2020, 57, 179-190.	1.9	21
67	Analyses of interfacial reactions at different levels of interconnection. Materials Science in Semiconductor Processing, 2004, 7, 307-317.	1.9	20
68	Thermodynamic modeling of Au–Ce–Sn ternary system. Calphad: Computer Coupling of Phase Diagrams and Thermochemistry, 2013, 42, 38-50.	0.7	20
69	Nanostructured Geometries Strongly Affect Fouling of Carbon Electrodes. ACS Omega, 2021, 6, 26391-26403.	1.6	20
70	Thermodynamic reassessment of Au–Cu–Sn ternary system. Journal of Alloys and Compounds, 2014, 588, 449-460.	2.8	19
71	What Does Nitric Acid Really Do to Carbon Nanofibers?. Journal of Physical Chemistry C, 2016, 120, 22655-22662.	1.5	19
72	Ultrathin undoped tetrahedral amorphous carbon films: thickness dependence of the electronic structure and implications for their electrochemical behaviour. Physical Chemistry Chemical Physics, 2015, 17, 9020-9031.	1.3	18

#	Article	IF	CITATIONS
73	Ultrathin undoped tetrahedral amorphous carbon films: The role of the underlying titanium layer on the electronic structure. Diamond and Related Materials, 2015, 57, 43-52.	1.8	18
74	Characterization and Electrochemical Properties of Oxygenated Amorphous Carbon (a-C) Films. Electrochimica Acta, 2016, 220, 137-145.	2.6	18
75	Redox Potentials from Ab Initio Molecular Dynamics and Explicit Entropy Calculations: Application to Transition Metals in Aqueous Solution. Journal of Chemical Theory and Computation, 2017, 13, 3432-3441.	2.3	18
76	Electrochemical detection of hydrogen peroxide on platinum-containing tetrahedral amorphous carbon sensors and evaluation of their biofouling properties. Materials Science and Engineering C, 2015, 55, 70-78.	3.8	17
77	Electrochemical Detection of Morphine in Untreated Human Capillary Whole Blood. ACS Omega, 2021, 6, 11563-11569.	1.6	17
78	Interfacial reactions in the Si/TaC/Cu system. Microelectronic Engineering, 2004, 71, 301-309.	1.1	16
79	Effect of Ti on the interfacial reaction between Sn and Cu. Journal of Materials Science: Materials in Electronics, 2012, 23, 68-74.	1.1	16
80	Thermal simulation of high-power Li-ion battery with LiMn1/3Ni1/3Co1/3O2 cathode on cell and module levels. International Journal of Energy Research, 2014, 38, 564-572.	2.2	16
81	Analysis of catechol, 4-methylcatechol and dopamine electrochemical reactions on different substrate materials and pH conditions. Electrochimica Acta, 2018, 292, 309-321.	2.6	16
82	Microstructural Evolution and Mechanical Properties of Au-20wt.%Sn Ni Interconnection. Journal of Electronic Materials, 2016, 45, 566-575.	1.0	15
83	Effect of Constant and Cyclic Current Stressing on the Evolution of Intermetallic Compound Layers. Journal of Electronic Materials, 2011, 40, 1517-1526.	1.0	14
84	Role of different factors affecting interdiffusion in Cu(Ga) and Cu(Si) solid solutions. Proceedings of the Royal Society A: Mathematical, Physical and Engineering Sciences, 2014, 470, 20130464.	1.0	13
85	Doping as a means to probe the potential dependence of dopamine adsorption on carbon-based surfaces: A first-principles study. Journal of Chemical Physics, 2017, 146, 234704.	1.2	13
86	Functionalized Nanocellulose/Multiwalled Carbon Nanotube Composites for Electrochemical Applications. ACS Applied Nano Materials, 2021, 4, 5842-5853.	2.4	13
87	Microstructural Evolution and Mechanical Properties in (AuSn)eut-Cu Interconnections. Journal of Electronic Materials, 2016, 45, 5478-5486.	1.0	12
88	Pt-grown carbon nanofibers for detection of hydrogen peroxide. RSC Advances, 2018, 8, 12742-12751.	1.7	12
89	Characterization and electrochemical properties of iron-doped tetrahedral amorphous carbon (ta-C) thin films. RSC Advances, 2018, 8, 26356-26363.	1.7	12
90	Reactive blending approach to modify spin-coated epoxy film: Part I. Synthesis and characterization of star-shaped poly(Iµ-caprolactone). Journal of Applied Polymer Science, 2006, 101, 3677-3688.	1.3	11

#	Article	IF	CITATIONS
91	Multi-walled carbon nanotubes (MWCNTs) grown directly on tetrahedral amorphous carbon (ta-C): An interfacial study. Diamond and Related Materials, 2015, 56, 54-59.	1.8	11
92	Fabrication of Micro- and Nanopillars from Pyrolytic Carbon and Tetrahedral Amorphous Carbon. Micromachines, 2019, 10, 510.	1.4	11
93	Biofouling affects the redox kinetics of outer and inner sphere probes on carbon surfaces drastically differently – implications to biosensing. Physical Chemistry Chemical Physics, 2020, 22, 16630-16640.	1.3	11
94	Amorphous carbon thin film electrodes with intrinsic Pt-gradient for hydrogen peroxide detection. Electrochimica Acta, 2017, 251, 60-70.	2.6	10
95	What Determines the Electrochemical Properties of Nitrogenated Amorphous Carbon Thin Films?. Chemistry of Materials, 2021, 33, 6813-6824.	3.2	10
96	Thermodynamic assessment of Au–La and Au–Er binary systems. Journal of Alloys and Compounds, 2011, 509, 4439-4444.	2.8	9
97	Diffusion and Growth of the μ Phase (Ni6Nb7) in the Ni-Nb System. Metallurgical and Materials Transactions A: Physical Metallurgy and Materials Science, 2011, 42, 1727-1731.	1.1	9
98	Thermodynamic assessment of Au–Ho and Au–Tm binary systems. Calphad: Computer Coupling of Phase Diagrams and Thermochemistry, 2012, 37, 87-93.	0.7	9
99	Energy band alignment and electronic states of amorphous carbon surfaces in vacuo and in aqueous environment. Journal of Applied Physics, 2015, 117, 034502.	1.1	9
100	The role of extra carbon source during the pre-annealing stage in the growth of carbon nanofibers. Carbon, 2016, 100, 351-354.	5.4	9
101	Hybrid X-ray Spectroscopy-Based Approach To Acquire Chemical and Structural Information of Single-Walled Carbon Nanotubes with Superior Sensitivity. Journal of Physical Chemistry C, 2019, 123, 6114-6120.	1.5	9
102	X-ray Spectroscopy Fingerprints of Pristine and Functionalized Graphene. Journal of Physical Chemistry C, 2021, 125, 18234-18246.	1.5	9
103	Effect of thickness and additional elements on the filtering properties of a thin Nafion layer. Journal of Electroanalytical Chemistry, 2019, 843, 12-21.	1.9	8
104	Rapid industrial scale synthesis of robust carbon nanotube network electrodes for electroanalysis. Journal of Electroanalytical Chemistry, 2021, 896, 115255.	1.9	8
105	Effect of oxygen on the reactions in Si/Ta/Cu and Si/TaC/Cu systems. Microelectronic Engineering, 2002, 64, 279-287.	1.1	7
106	Improving the function of dopamine electrodes with novel carbon materials. , 2013, 2013, 632-4.		7
107	Thermodynamics, Phases, and Phase Diagrams. , 2014, , 1-86.		7
108	The Combined Effect of Shock Impacts and Operational Power Cycles on the Reliability of Handheld Device Component Board Interconnections. Journal of Electronic Materials, 2012, 41, 3232-3246.	1.0	6

#	Article	IF	CITATIONS
109	Effect of Isothermal Aging and Electromigration on the Microstructural Evolution of Solder Interconnections During Thermomechanical Loading. Journal of Electronic Materials, 2012, 41, 3179-3195.	1.0	6
110	Effect of Power Density on the Electrochemical Properties of Undoped Amorphous Carbon (aâ \in C) Thin Films. Electroanalysis, 2019, 31, 746-755.	1.5	6
111	Nanoscale geometry determines mechanical biocompatibility of vertically aligned nanofibers. Acta Biomaterialia, 2022, 146, 235-247.	4.1	6
112	Effect of isothermal annealing and electromigration pre-treatments on the reliability of solder interconnections under vibration loading. Journal of Materials Science: Materials in Electronics, 2013, 24, 644-653.	1.1	5
113	Understanding the Growth of Interfacial Reaction Product Layers between Dissimilar Materials. Critical Reviews in Solid State and Materials Sciences, 2016, 41, 73-105.	6.8	5
114	Reliability of Tantalum Based Diffusion Barriers between Cu and Si. Materials Research Society Symposia Proceedings, 2000, 612, 741.	0.1	4
115	Phase Evolution in the AuCu/Sn System by Solid-State Reactive Diffusion. Journal of Electronic Materials, 2014, 43, 3357-3371.	1.0	4
116	Defects, Driving Forces and Definitions of Diffusion Coefficients in Solids. , 2017, , 1-54.		4
117	Effect of Electrochemical Oxidation on Physicochemical Properties of Feâ€Containing Singleâ€Walled Carbon Nanotubes. ChemElectroChem, 2020, 7, 4136-4143.	1.7	4
118	Evaluation of electrolessly deposited NiP integral resistors on flexible polyimide substrate. Microelectronics Reliability, 2005, 45, 665-673.	0.9	3
119	Reactive blending approach to modify spin-coated epoxy film: Part II. Crosslinking kinetics. Journal of Applied Polymer Science, 2006, 101, 3689-3696.	1.3	3
120	A Comparative Study of Power Cycling and Thermal Shock Tests. , 2006, , .		3
121	Interfacial Adhesion in Polymer Systems. Microsystems, 2012, , 101-133.	0.3	3
122	Development of Interdiffusion Zone in Different Systems. , 2014, , 141-166.		3
123	Hybrid carbon nanomaterials for electrochemical detection of biomolecules. Physica Scripta, 2015, 90, 094006.	1.2	3
124	In-situ functionalization of tetrahedral amorphous carbon by filtered cathodic arc deposition. AIP Advances, 2019, 9, 085325.	0.6	3
125	Time-Based Sensor Interface for Dopamine Detection. IEEE Transactions on Circuits and Systems I: Regular Papers, 2020, 67, 3284-3296.	3.5	3
126	Thermal investigation of a battery module for work machines. , 2011, , .		2

#	Article	IF	CITATIONS
127	Comments on "Effects of current density on the formation and microstructure of Sn–9Zn, Sn–8Zn–3Bi and Sn–3Ag–0.5Cu solder joints― Intermetallics, 2012, 28, 164-165.	1.8	2
128	Connection between the physicochemical characteristics of amorphous carbon thin films and their electrochemical properties. Journal of Physics Condensed Matter, 2021, 33, 434002.	0.7	2
129	Analysis of microstructural evolution in SLID-bonding used for hermetic encapsulation of MEMS devices. , 2012, , .		1
130	Interdiffusion and the Kirkendall Effect in Binary Systems. , 2014, , 239-298.		1
131	Thermodynamic-Kinetic Method on Microstructural Evolutions in Electronics. , 2017, , 101-147.		1
132	A Sensor Interface for Neurochemical Signal Acquisition. , 2019, , .		1
133	Introduction to Thermodynamic-Kinetic Method. Microsystems, 2012, , 45-100.	0.3	1
134	Understanding materials compatibility issues in electronics packaging. , 2009, , .		0
135	On the role of electromigration in power cycling tests. , 2010, , .		0
136	Study on the Growth of Nb ₃ Sn Superconductor in Cu(Sn)/Nb Diffusion Couple. Defect and Diffusion Forum, 2010, 297-301, 467-471.	0.4	0
137	Interfacial reactions between SnAg1.0Ti and Ni metallization. Journal of Materials Science: Materials in Electronics, 2012, 23, 2030-2034.	1.1	0
138	Finite element modeling for reliability assessment of solder interconnections in a power transistor. , 2012, , .		0
139	Simulation of Dynamic Recrystallization in Solder Interconnections During Thermal Cycling. , 2013, , .		0
140	Understanding the effect of electromigration on the growth of interfacial reaction layers in Cu-Sn and Cu-Ni-Sn systems. , 2014, , .		0
141	Evolution of Different Types of Interfacial Structures. Microsystems, 2012, , 135-211.	0.3	0
142	Undoped Tetrahedral Amorphous Carbon (ta-C) Thin Films for Biosensing. , 2020, , 11-1-11-15.		0
143	Carbonaceous Nanomaterials for Electrochemical Biosensing. , 2022, , .		Ο